Fractal analysis of chaotic tunneling of squeezed states in a double-well potential

Article *in* Physical Review A · March 1987

DOI: 10.1103/PhysRevA.35.1825 · Source: PubMed

1 author:

Hans Dekker
University of Amsterdam
177 PUBLICATIONS **2,550** CITATIONS

SEE PROFILE

Fractal analysis of chaotic tunneling of squeezed states in a double-well potential

H. Dekker
Physics & Electronics Laboratory (FEL), Netherlands Organisation for Applied Scientific Research (TNO), Postbox 96864, The Hague, The Netherlands
(Received 24 March 1986)

The exponentially small energy-level splittings $\Delta E_{2n} \equiv E_{2n+1} - E_{2n}$ ($n = 0, 1, \ldots$) for ground-state as well as excited-state doublets in a symmetric bistable potential are determined by means of a simple explicit formula. The tunneling frequencies $\Delta\omega_{2n} \equiv \Delta E_{2n}/\hbar$ form a quasi-Weierstrass spectrum, which explains the erratic tunneling behavior of an initially squeezed wave packet. It also implies the existence of a natural fractal (Hausdorff-Besicovitch) dimension D for the chaotic tunneling trajectory, as is shown by computerized zooming towards the picture of position versus time and determining (over a fixed period of time, with sampling time intervals Δt varying over more than four orders of magnitude) the total sample path length $L \sim (\Delta t)^{1-D}$.

I. INTRODUCTION

Let a nonrelativistic quantum-mechanical particle (of unit mass, for convenience) be subjected to a field of force derivable from a one-dimensional potential $U(x)$. That is, the particle's dynamics is dictated by the Schrödinger equation

$$\tfrac{1}{2}\hbar^2\psi''(x) + [E - U(x)]\psi(x) = 0 \tag{1.1}$$

for the eigenfunctions $\psi(x)$ with energy E, the prime denoting differentiation with respect to position x. Now let the potential be characterized by two identical minima [or potential holes, located at $x = \pm a$ where $U(a) \approx \frac{1}{2}\omega_0^2(x \pm a)^2$] separated by a potential barrier of height U_0 (located at $x = 0$). See Fig. 1. Typical examples of symmetric double-well potentials are the double oscillator[1] and the quartic potential (see, e.g., Ref. 2). For such a potential the spectrum is discrete and bounded from below, so that the energy eigenvalues can be properly labeled by $n = 0, 1, 2, \ldots$. That is, E_n is the eigenvalue belonging to the eigenfunction $\psi_n(x)$.

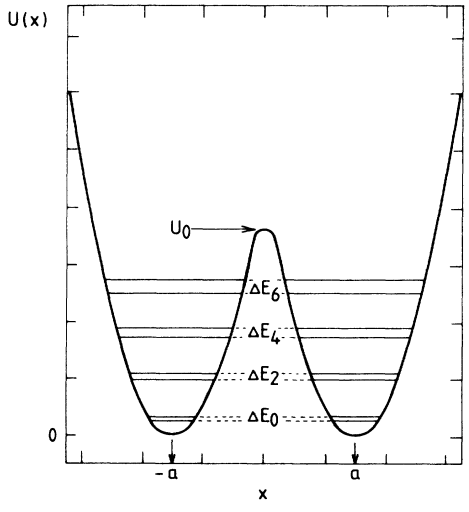

FIG. 1. Typical globally symmetric bistable potential $U(x)$ relevant to the problem of coherent tunneling.

If the barrier were infinitely high (and of nonzero width), the potential holes would be noninteracting and the energy spectrum of the total system would be doubly degenerate. However, once the barrier becomes finite, the holes become interacting by means of coherent tunneling through the barrier. In consequence, the degeneracy is lifted and doublets show up with a level splitting $\Delta E_{2n} \equiv E_{2n+1} - E_{2n}$. If at time $t = 0$ the particle is localized in one of the two potential wells such that the initial wave packet only involves the lowest-lying doublet (i.e., $n = 0$), then the particle coheres back and forth between the holes as

$$x(t) = x(0)\cos(\Delta\omega_0 t) , \tag{1.2}$$

where $x(0) = \pm a$ and $\Delta\omega_0 \equiv \Delta E_0/\hbar$, as is well known from the classic example of the ammonia inversion.[1,3,4]

Let the particle be present on the left-hand side of the barrier, i.e., in well A. If the motion in the well can be treated classically, the particle will strike the barrier at a mean rate $\omega_0/2\pi$ (where $\omega_0 \gg \Delta\omega_0$ is the frequency of local oscillations at the minima). Now, stochastic interruption of the coherent probability amplitude for finding the particle in well A,

$$\psi_A(t) = \cos(\tfrac{1}{2}\Delta\omega_0 t) , \tag{1.3}$$

at this classical rate,[5-7] i.e., with time intervals $\Delta t = 2\pi/\omega_0$, would at time $t = N\Delta t$ yield the incoherent amplitude

$$\psi_A(t \mid \Delta t) \equiv \prod_{n=1}^{N} \cos(\tfrac{1}{2}\Delta\omega_0 \Delta t) \approx \prod_{n=1}^{N} [1 - \tfrac{1}{2}(\tfrac{1}{2}\Delta\omega_0 \Delta t)^2]$$
$$\approx \exp\left[-\tfrac{1}{8}(\Delta\omega_0)^2 \sum_{n=1}^{N} (\Delta t)^2 \right] \equiv \exp(-\tfrac{1}{2}\kappa_0 t) , \tag{1.4}$$

where $\kappa_0 \equiv \pi(\Delta\omega_0)^2/2\omega_0$. Hence, one would obtain $P_A(t \mid \Delta t) = \exp(-\kappa_0 t)$ for the probability to find the particle in the initial well. Clearly, κ_0 is the escape rate.

However, the rate of escape via incoherent tunneling through a barrier can also be found by the following reasoning.[8] Let the particle again attempt to penetrate the barrier at the mean classical rate $\omega_0/2\pi$. And for the probability of a successful tunneling attempt let us take the standard textbook WKB transmission probability $T_0^2=\exp(-2S_0/\hbar)$ for free-particle tunneling, where S_0 is the classical Euclidean action-integral (i.e., in the inverted potential) across the barrier.[1,8,9] Hence, $\kappa_0=\omega_0 T_0^2/2\pi$. Comparing the two obtained expressions for κ_0, one readily finds

$$\Delta\omega_0^{\mathrm{WKB}}=(\omega_0/\pi)e^{-S_0/\hbar}, \tag{1.5}$$

which is indeed the correct semiclassical formula.[3,8,10]

There is an elegant—equally heuristic—alternative argument to gather the above result. Namely, if again $\psi_A(t)=\cos(\frac{1}{2}\Delta\omega_0 t)$, then using the conservation of probability, i.e., $|\psi_A(t)|^2+|\psi_B(t)|^2=1$, one obtains $|\psi_B(t)|=|\sin(\frac{1}{2}\Delta\omega_0 t)|$. Hence, in those periods when there is a net flow from A to B, one has $|\psi_B(t)|^{\bullet}=\frac{1}{2}\Delta\omega_0|\psi_A(t)|$, the dot denoting differentiation with respect to time. In particular, $|\psi_B(+0)|^{\bullet}=\frac{1}{2}\Delta\omega_0|\psi_A(+0)|$. But this time rate of change of the amplitude to find the particle on the other side of the barrier can also be found in another way, analogous to that of the preceding paragraph. Once more, let the particle initially be in well A, let it attempt to penetrate the barrier at the classical rate $\omega_0/2\pi$, and let us take the standard WKB formula $T_0=\exp(-S_0/\hbar)$ for the transmission amplitude. Then $|\psi_B(+0)|^{\bullet}=(\omega_0 T_0/2\pi)|\psi_A(+0)|$, and comparing this with the previous expression again yields the correct semiclassical result (1.5).

In view of the simplicity of the above arguments, it is somewhat astonishing that this important result (not only for molecular inversion spectra, but also, e.g., for the promising paradigm of macroscopic quantum coherence in dissipation-free superconducting interference devices[6,7,10–13]) is not discussed in the standard literature, with the notable exception of Landau and Lifshitz's textbook on quantum mechanics.[8] Only one more topical monograph[14] dealing with the WKB formula for the level splitting (and making reference to an original paper by Dennison and Uhlenbeck[3]) has come to my attention. In fact, the truly interesting result providing the general and exact exponential prefactor (rather than the semiclassical value ω_0/π) does not seem to be readily available. Merzbacher,[1] though, has considered the exact double harmonic oscillator—in particular, its ground-state level splitting—whereas Coleman[15] discussed a more general barrier by means of the instanton method,[16–18] again only for the ground-state doublet. However, if the initial wave packet—prepared in either potential hole—is squeezed[19–21] in its width in comparison to the local ground-state Gaussian, the higher-lying energy-level splittings will be necessarily involved in the ensuing tunneling dynamics.

Therefore, in Sec. II the higher tunneling frequencies $\Delta\omega_{2n}\equiv\Delta E_{2n}/\hbar$ are determined by means of an elementary, explicit and exact formula for the energy-level splittings, rather than by applying some generalized form of the instanton calculation, which seems to be too awkward for the present problem.[15,22] Then the tunneling propagator[1,23,24] is constructed, yielding in particular the expectation value $x(t)$. Although $x(t)$ throughout will be given by an apparently simple coherent (i.e., nonstochastic, nondissipative) superposition of cosine functions, the tunneling spectrum is such that sampling the expected position of the particle as a function of time reveals substantial chaotic[25–28] tunneling features upon squeezing the initial wave packet. This is shown in Sec. III, which also contains a discussion of $x(t)$ as a natural (or physical, as opposed to a mathematically exact) fractal function.[29] Some summarizing remarks are made in Sec. IV.

II. TUNNELING DYNAMICS

A. The eigenfunctions

Let the barrier be sufficiently high, i.e., $U_0\gg\hbar\omega_0$, such that it is allowed to employ WKB wave functions[1,8,9] within the barrier peak region (near $x=0$) for all pertinent doublets. As usual, defining (for a particle of unit mass)

$$\kappa(x)\equiv\sqrt{2[U(x)-E]}, \tag{2.1}$$

the unnormalized WKB solutions of (1.1) read

$$\psi(x)=[\kappa(x)]^{-1/2}\exp\left[\pm\int_0^x\kappa(x')dx'/\hbar\right]. \tag{2.2}$$

Near the top of the barrier one then considers the approximation[15]

$$\kappa(x)\approx\sqrt{2U(x)}-E/\sqrt{2U(x)}. \tag{2.3}$$

In the integral in the exponentials in (2.2) it is required—in view of the factor $1/\hbar$—to carry both terms from (2.3) along to obtain the correct upshot for the prefactor through leading order in $\hbar\omega_0/U_0\ll 1$, while in the remainder of (2.2)—i.e., in $\kappa(x)^{-1/2}$—it suffices to keep the first term only. One thus obtains

$$\psi(x)=[2U(x)]^{-1/4}\times\exp\left[\pm\left[\int_0^x\sqrt{2U(x')}dx'-E\int_0^x dx'/\sqrt{2U(x')}\right]\Big/\hbar\right]. \tag{2.4}$$

Now introducing the abbreviations

$$S(x)\equiv\int_{-x}^{x}\sqrt{2U(x')}dx',\quad \tau(x)\equiv\int_0^x dx'/\sqrt{2U(x')}, \tag{2.5}$$

substituting for E the degenerate values $E_{2n+1}\approx E_{2n}\approx(n+\frac{1}{2})\hbar\omega_0$— which is correct to leading order in $\hbar\omega_0/U_0\ll 1$—and explicitly constructing from (2.4) the globally even and odd solutions, one may write the result as

$$\begin{aligned}\psi_{2n}(x)&=[2U(x)]^{-1/4}\cosh[-(n+\tfrac{1}{2})\omega_0\tau(x)+\tfrac{1}{2}S(x)/\hbar],\\ \psi_{2n+1}(x)&=[2U(x)]^{-1/4}\sinh[-(n+\tfrac{1}{2})\omega_0\tau(x)+\tfrac{1}{2}S(x)/\hbar],\end{aligned} \tag{2.6}$$

with $n=0,1,2,\ldots$.

Because of the symmetry of the problem, we may restrict further considerations to positive x. Let then $x \uparrow a$, i.e., towards the right-hand potential well B of Fig. 1. Obviously, the two exponentials in the hyperbolic functions in (2.6) become asymptotically differing in order of magnitude by the enormous factor $\exp(S_0/\hbar)$, where $S_0 \equiv S(a)$. Fortunately, anticipating the use of the perfectly tailored formula (2.11) for the level splitting in Sec. II B, it suffices to merely keep the leading exponential, i.e., $\exp(\frac{1}{2}S_0/\hbar)$. In the parabolic region $U(x) \approx \frac{1}{2}\omega_0^2(x-a)^2$, so that $\sqrt{2U(x)} \approx \omega_0(a-x)$ when $x \uparrow a$. Introducing this asymptotic behavior into (2.5), one finds

$$S(x) \overset{x \uparrow a}{\longrightarrow} S_0 - \omega_0(a-x)^2 , \tag{2.7}$$

$$\tau(x) \overset{x \uparrow a}{\longrightarrow} \tau_0 - \omega_0^{-1}\ln[(a-x)/a] . \tag{2.8}$$

The latter formula implicitly defines the time constant τ_0, which may be interpreted as the time it takes to travel from $x=0$ to the parabolic well region. Indeed, for the exact double oscillator $\tau_0=0$. It is noted in passing that $2\tau_0$ coincides with the instanton lifetime.[15] The general existence of this quantity is easily proved introducing a $\tau_0(x)$ by defining (2.8) to be valid for all $x<a$, using (2.5) for $\tau(x)$, and investigating the derivative $\tau_0'(x)$ when $x \uparrow a$.

Returning to (2.6) armed with the knowledge of the preceding paragraph, and introducing the usual local coordinate $\eta \equiv \sqrt{\omega_0/\hbar}(x \pm a)$, one easily observes that on approach of the potential minimum the asymptotic behavior of the eigenfunctions is given by

$$\psi_{2n}(x) \approx \tfrac{1}{2}(a\omega_0)^{-1/2}\left[\frac{\eta}{a}\left[\frac{\hbar}{\omega_0}\right]^{1/2}\right]^n \times \exp[-\tfrac{1}{2}\eta^2 - (n+\tfrac{1}{2})\omega_0\tau_0 + \tfrac{1}{2}S_0/\hbar] ,$$
$$\psi_{2n+1}(x) \approx \psi_{2n}(x) . \tag{2.9}$$

Let us now recall that these wave functions belong to the nth excited doublet, which involves the nth excited degenerate energy levels $E_{2n+1} \approx E_{2n} \approx (n+\frac{1}{2})\hbar\omega_0$. Therefore, it is indeed no coincidence that the asymptotic barrier functions (2.9) nicely connect in a smooth manner with the asymptotic form of the pertinent local harmonic-oscillator eigenfunctions. Namely[1,8,9] the latter are proportional to $H_n(\eta)\exp(-\frac{1}{2}\eta^2)$, where $H_n(\eta)$ represents the nth-degree Hermite polynomial, and $H_n(\eta) \approx (2\eta)^n$ when $\eta \to \pm\infty$. Hence, the appropriate eigenfunctions in the well region—corresponding to (2.6)—can be specified as

$$\psi_{2n}(x) = \tfrac{1}{2}(a\omega_0)^{-1/2}\left[\frac{1}{2a}\left[\frac{\hbar}{\omega_0}\right]^{1/2}\right]^n H_n(\eta) \times \exp[-\tfrac{1}{2}\eta^2 - (n+\tfrac{1}{2})\omega_0\tau_0 + \tfrac{1}{2}S_0/\hbar] ,$$
$$\psi_{2n+1}(x) = \psi_{2n}(x) . \tag{2.10}$$

The expressions (2.6) for the nth excited doublet eigenfunctions in the barrier peak region and (2.10) for the corresponding eigenfunction in the potential-well region suffice for the evaluating of the energy-level splitting by means of the formula in Sec. II B.

B. The level splitting

Consider the Schrödinger equation (1.1) for $\psi_{2n}(x)$, with energy E_{2n}, and multiply it by $\psi_{2n+1}(x)$. Similarly, multiply (1.1) for $\psi_{2n+1}(x)$, with energy E_{2n+1}, by $\psi_{2n}(x)$. Subtract the two resulting expressions and integrate over $x \in [0,\infty)$. In view of the properties of $U(x)$—in particular $U(\infty)=\infty$ and $U(-x) \equiv U(x)$—the wave functions tend rapidly to zero at infinity, while at the origin one has $\psi_{2n}'(0)=\psi_{2n+1}(0)=0$. Thus one obtains the explicit and exact expression

$$\Delta E_{2n} = \tfrac{1}{2}\hbar^2[\psi_{2n}(0)\psi_{2n+1}'(0)] \Big/ \left[\int_0^\infty \psi_{2n}(x)\psi_{2n+1}(x)dx\right] \tag{2.11}$$

for the level splitting. This formula is perfectly tailored to the problem as its numerator is entirely fixed by the nature of the wave functions at the very top of the barrier, while its denominator is essentially determined by their properties in the wells. Note that by (2.11) one directly obtains the splitting itself rather than calculating it as a correction term which is exponentially small compared to uncomputed nonexponential corrections to the degenerate energy values. From a purist point of view the validity of the latter method is not obvious.[15] It also depends on much more subtle details of the connection procedure for the eigenfunctions than the present method.

From (2.6) one has

$$\psi_{2n}(0) = (2U_0)^{-1/4}, \quad \psi_{2n+1}'(0) = (2U_0)^{1/4}/\hbar , \tag{2.12}$$

where in $\psi_{2n+1}'(0)$, terms of relative order $\hbar\omega_0/U_0 \ll 1$ have been disregarded. Similarly, neglecting exponentially small corrections, from (2.10) one gets

$$\int_0^\infty \psi_{2n}(x)\psi_{2n+1}(x)dx = \frac{1}{2\omega_0}\left[\frac{e^{-\omega_0\tau_0}}{2a}\left[\frac{\hbar}{\omega_0}\right]^{1/2}\right]^{2n+1} e^{S_0/\hbar} \times \int_{-\infty}^{\infty} H_n^2(\eta)e^{-\eta^2}d\eta . \tag{2.13}$$

Using, e.g., formula 7.374.1 from Ref. 30 to infer the value $2^{2n}n!\sqrt{\pi}$ for the integral over η, and inserting (2.13) and (2.12) into (2.11), the final result for $\Delta\omega_{2n} \equiv \Delta E_{2n}/\hbar$ is easily cast into the form

$$\Delta\omega_{2n} = (\bar{\omega}_{2n}/\pi)e^{-S_0/\hbar} , \tag{2.14}$$

where the "attempt" frequency for the nth excited doublet is given by

$$\bar{\omega}_{2n} = \bar{\omega}_0(ae^{\omega_0\tau_0}\sqrt{2\omega_0/\hbar})^{2n}/n! , \tag{2.15}$$

and where the ground-state doublet's value reads

$$\bar{\omega}_0 = 2a\omega_0 e^{\omega_0\tau_0}\sqrt{\pi\omega_0/\hbar} . \tag{2.16}$$

As it should, this $\bar{\omega}_0$ agrees with the result of Ref. 22. It also coincides with the upshot from the instanton method,[15] and for the exact double oscillator it agrees with Ref. 1. Together with the degenerate values $E_{2n+1} \approx E_{2n} \approx (n+\frac{1}{2})\hbar\omega_0$ the novel formula (2.14) determines the energy spectrum relevant for the tunneling dynamics, as will be disussed in Sec. II C.

C. The tunneling propagator

The quantum-mechanical propagator[1,23,24,31] for the problem posed by the Schrödinger equation (1.1) may be given as

$$K(x,t \mid x',0)=\sum_{n=0}^{\infty} \psi_n(x)\psi_n^*(x')e^{-iE_n t/\hbar} \tag{2.17}$$

if $t \geq 0$, while $K(x,t \mid x',0) \equiv 0$ if $t<0$. By means of (2.17) the time evolution of any initial wave packet $\phi(x)$ follows from the integral equation

$$\varphi(x,t)=\int_{-\infty}^{\infty} K(x,t \mid x',0)\varphi(x')dx' . \tag{2.18}$$

For $\phi(x)$ let us take the Gaussian wave packet

$$\varphi(x)=(\pi\hbar e^{-2R}/\omega_0)^{-1/4}\exp(-\tfrac{1}{2}\eta^2 e^{2R}) , \tag{2.19}$$

which is centered at a potential minimum, and where R is the squeezing parameter.[20] Inserting (2.19) into (2.18), invoking (2.17) for the kernel and using the properly normalized globally even or odd combination of the local form (2.10) for the eigenfunctions, one obtains

$$\varphi(x,t)=\sum_{n=0}^{\infty} A_n[\psi_{2n}(x)e^{-iE_{2n}t/\hbar} + \psi_{2n+1}(x)e^{-iE_{2n+1}t/\hbar}] , \tag{2.20}$$

where

$$A_n \equiv (e^R/\pi 2^{n+1}n!)^{1/2}\int_{-\infty}^{\infty} H_n(\eta)e^{-(1+e^{2R})\eta^2/2}d\eta . \tag{2.21}$$

Obviously, as a consequence of the symmetry of the initial wave packet about $\eta=0$, all odd-indexed $A_{2n+1}=0$. By means of formula 7.373.2 (or 7.374.4) from Ref. 30, one finds for the even-indexed coefficients

$$A_{2n}=[\sqrt{(2n)!}(\tfrac{1}{2}\tanh R)^n]/(n!\sqrt{2\cosh R}) . \tag{2.22}$$

From (2.20) the probability density $P(x,t) \equiv \mid \phi(x,t) \mid^2$ is now readily used to calculate the chances of finding the particle in the A (or B) well by integrating $P(x,t)$ over $x \in (-\infty,0)$ [or $x \in (0,\infty)$]. Which is the initial well is determined now in (2.20) by the choice of the relative sign of $\psi_{2n}(x)$ and $\psi_{2n+1}(x)$. Let then

$$P_0(t) \equiv \int_{x \in \text{initial well}} \mid \varphi(x,t) \mid^2 dx \tag{2.23}$$

denote the probability to still (or again) find the particle in the initial well. Once more using the form (2.10) of the eigenfunctions in the potential wells and noticing the standard orthogonality properties of the Hermite polynomials[30,32,33] the result reads

$$P_0(t)=\sum_{n=0}^{\infty} 2A_{2n}^2\cos^2(\tfrac{1}{2}\Delta\omega_{4n}\, t) . \tag{2.24}$$

Using either a binomial series or—noticing that $(2n)!/n!=2^{2n}(\frac{1}{2})_n$, where $(\frac{1}{2})_n$ is a Pochhammer symbol—invoking a standard result (e.g., formula 15.1.8 from Ref. 32) from the theory of hypergeometric functions, and employing an elementary formula for hyperbolic functions, it is easily checked that the right-hand side of (2.24) indeed sums up to unity at $t=0$, as it should. Furthermore, from (2.22) one readily infers that at zero squeezing (i.e., ground-state doublet tunneling) $A_{2n\neq 0}=0$ while $A_0=1/\sqrt{2}$, so that in that case (2.24) properly reduces to the well known single cosine. Assuming then the particle to start in the A-well, say, and putting $P_0(t) \equiv \mid \psi_A(t) \mid^2$ one recovers the probability amplitude $\psi_A(t)$ mentioned in the Introduction.

Multiplying $P(x,t)$ by x and integrating over all $x \in (-\infty,\infty)$ one obtains the expected position $x(t)$ (quantum-mechanical brackets are conveniently suppressed here). Alternatively, which is identical at least to leading order in $\hbar\omega_0/U_0 \ll 1$, one might argue that whereas x has the probability $P_0(t)$ given in (2.24) to achieve the initial value $x(0)=\pm a$, it has the probability $1-P_0(t)$ to acquire the opposite value $-x(0)$ pertinent to the other well. Hence, using (2.24) one obtains

$$x(t)/x(0)=\sum_{n=0}^{\infty} 2A_{2n}^2\cos(\Delta\omega_{4n}\, t) . \tag{2.25}$$

This fairly simple formula for the expected position as a function of time will be discussed in much greater detail in Sec. III.

III. DISCUSSION

A. Chaotic behavior

An obviously interesting question is: What does the expected trajectory $x(t)$ look like when the initial wave packet is squeezed (i.e., $R \neq 0$)? The precise answer turns out to be as intricate as the question is obvious. Let us rewrite (2.25) in terms of a time scale where $\Delta\omega_0$ equals unity. Then, again denoting time by t, we have

$$x(t)/x(0)=\sum_{n=0}^{\infty} a_n\cos\Omega_n t , \tag{3.1}$$

$$a_n \equiv [(2n)!(\tfrac{1}{2}\tanh R)^{2n}]/[(n!)^2\cosh R] , \tag{3.2}$$

$$\Omega_n \equiv \beta^{2n}/(2n)!, \quad \beta \equiv (2a^2\omega_0/\hbar)e^{2\omega_0\tau_0} . \tag{3.3}$$

The parameter β defined in (3.3) essentially measures the height of the barrier. As mentioned before, for the typical case of the double harmonic oscillator $\tau_0=0$ while $U_0=\frac{1}{2}\omega_0^2 a^2$, so that $\beta=4U_0/\hbar\omega_0$. Indeed, in general $\beta \gg 1$. The consequently rather large ratios of tunneling frequencies obviously make it virtually impracticable to draw a picture of x versus t by hand, in particular at somewhat stronger squeezing where the higher frequencies contribute significantly. In fact, it would be difficult to decide where to stop improving the sampling rate other than at a value which is much larger than the highest

relevant frequency Ω_N. Even with machine calculations this becomes prohibitive. For example, if $\beta=48$ then Ω_6 is already of the order of 10^{12}, which is at the limit of standard single-precision arithmetic.

Obviously, even in the computer calculations one should set rather severe restrictions on the allowed values of β, on the number N of terms to be carried along in (3.1), and on the squeezing R. These restrictions are not independent of one another. In fact, already from an analytical point of view the summation in (3.1) should be handled cautiously. Namely, even for the perfect double oscillator, the formula of Sec. II for the tunneling spectrum can be expected to fail for levels up from the barrier peak, essentially because in many places the proper expansion parameter is $n\hbar\omega_0/U_0$ rather than $\hbar\omega_0/U_0 \ll 1$ itself. This certainly limits the significant values of n, although from Appendix A one might acquire confidence in the validity of our formula even for the high-lying doublets.

Since the n-labeled term in (3.1) involves the $2n$th excited doublet, it is related to the degenerate energies $E_{4n} \approx E_{4n+1} \approx (2n+\frac{1}{2})\hbar\omega_0$. Using again $\beta=4U_0/\hbar\omega_0$, anticipating $N \gtrsim 1$ and requiring $E_{4N} \lesssim U_0$, one finds the constraint $N \lesssim \frac{1}{8}\beta$. On the other hand, cutting off the series will be allowed only if the sum of the disregarded terms indeed does not contribute appreciably to the total result. Tentatively keeping the total energy $E(R)=\frac{1}{2}\hbar\omega_0\cosh(2R)$ below the barrier peak energy U_0, one arrives at the constraint $R \lesssim \frac{1}{2}\operatorname{arccosh}(\frac{1}{2}\beta)$ on the

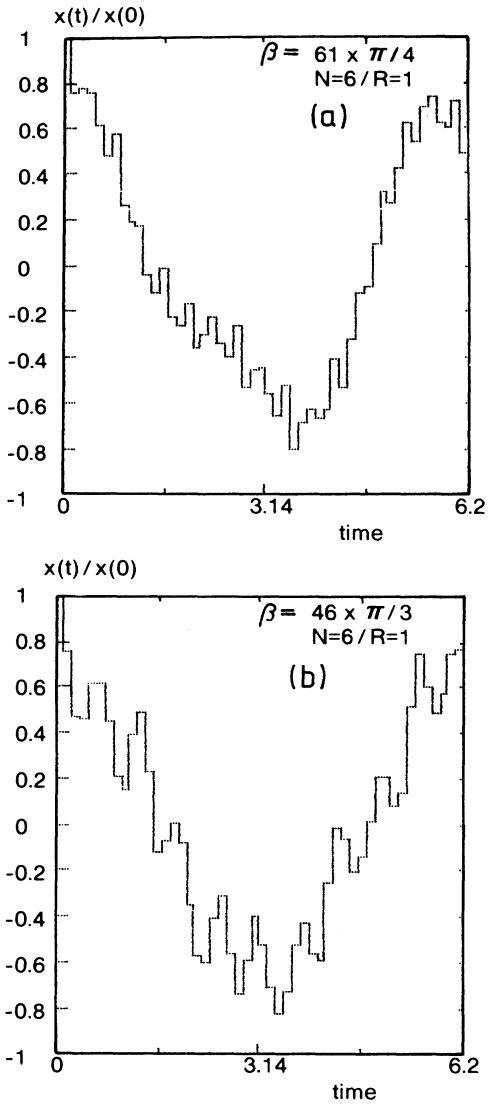

FIG. 2. Expected normalized position vs time of a particle tunneling in a symmetric bistable potential, according to formulas (3.1)—(3.3). $N=6$ is the number of terms in the sum in (3.1) carried along in the computer calculations. $R=1$ specifies the squeezing of the initial wave packet (2.19). The sampling time interval is $\Delta t=\pi/25$ in units where the ground-state level-splitting frequency $\Omega_0 \equiv 1$. The parameter β defined in (3.3) essentially indicates the height of the barrier; (a) $\beta=61\pi/4 \approx 47.9093$, (b) $\beta=46\pi/3 \approx 48.1711$.

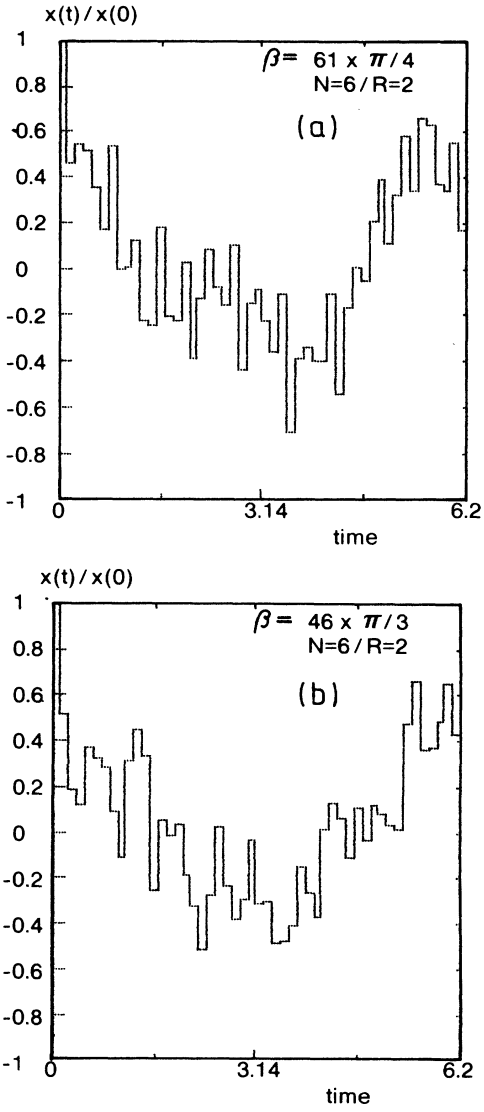

FIG. 3. Like Fig. 2, but for increased squeezing $R=2$.

amount of squeezing. Alternatively, one might calculate the finite sum in (3.1) at $t=0$. For finite N letting $R\to\infty$, the sum tends to zero inversely proportional to $\cosh R$. The constant of proportionality can be found as follows. Differentiate the finite sum with respect to $\tanh^2 R$ and construct a simple first-order differential equation for it. Solving this equation one obtains the exact result

$$x_N(0)/x(0)=I_{1-\tanh^2 R}(\tfrac{1}{2},N)\ , \tag{3.4}$$

where $I_{1-z}(\nu,\mu)\equiv 1-I_z(\mu,\nu)$ with $I_z(\mu,\nu)\equiv B_z(\mu,\nu)/B(\mu,\nu)$ being the normalized incomplete beta function (see, e.g., Ref. 32 formula 26.5.6). Thus one finds the aforementioned proportionality factor to be $2\sqrt{N/\pi}$ if $N\gg 1$. Hence, keeping $x_N(0)/x(0)\approx 1$ leads to $N\approx(\pi/4)\cosh^2 R$. Combining this with $N\lesssim\frac{1}{8}\beta$, one obtains $R\lesssim\operatorname{arccosh}(\sqrt{\beta/2\pi})$, which for the pertinent β values is almost equally restrictive as the previous constraint.

The computer calculations for $x(t)$ have been performed on a Hewlett Packard HP85 (connected to a standard HP matrix printer for producing the figures), which has a single precision of 12 decimal digits. Hence, the largest argument in the cosines in (3.1) had to be less than 10^{13}. Using $N\approx\frac{1}{8}\beta$, we have therefore required N to be the largest integer fulfilling $2\pi\Omega_N\approx 2\pi(8N)^{2N}/(2N)!\lesssim 10^{13}$. This condition is met up to $N=6$, which has indeed been taken as the maximum number of terms to be carried along in (3.1). Consequently, $\beta\approx 48$. Special attention has been given to the irrational (choice of) values $\beta=61\pi/4\approx 47.9093$ and $\beta=46\pi/3\approx 48.1711$. The squeezing is limited to $R\approx\frac{1}{2}\operatorname{arccosh}(\frac{1}{2}\beta)\lesssim 2$.

In Fig. 2 the function $x(t)/x(0)$ has been computed over the first fundamental period $t\in[0,2\pi]$ for $R=1$ and (a) $\beta=61\pi/4$, (b) $\beta=46\pi/3$, with 51 sample points so that the sampling time interval is $\Delta t=\pi/25$. Figure 3 has the same legend as Fig. 2, but for $R=2$. If $R=0$ (no squeezing, i.e., ground-state tunneling) these figures would

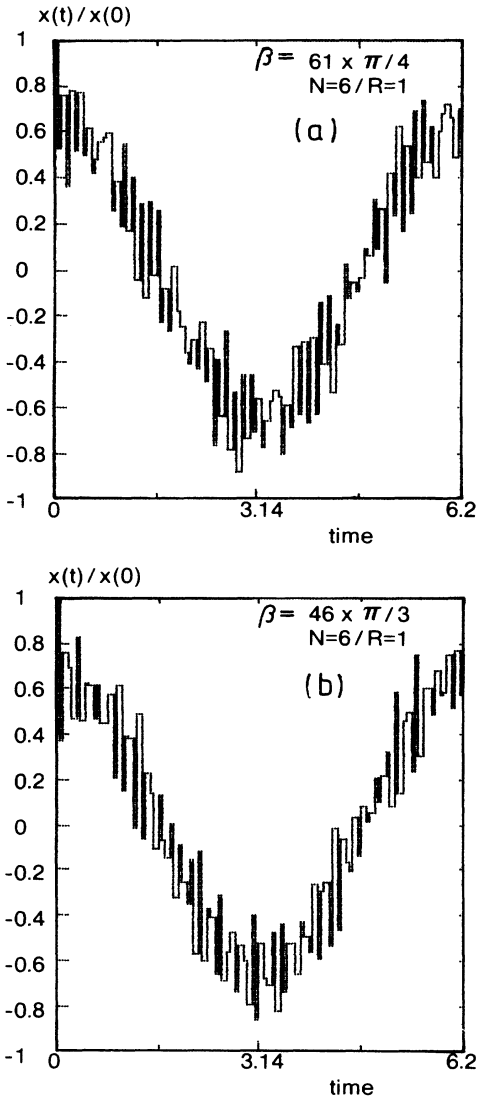

FIG. 4. Like Fig. 2, but for decreased $\Delta t=\pi/50$.

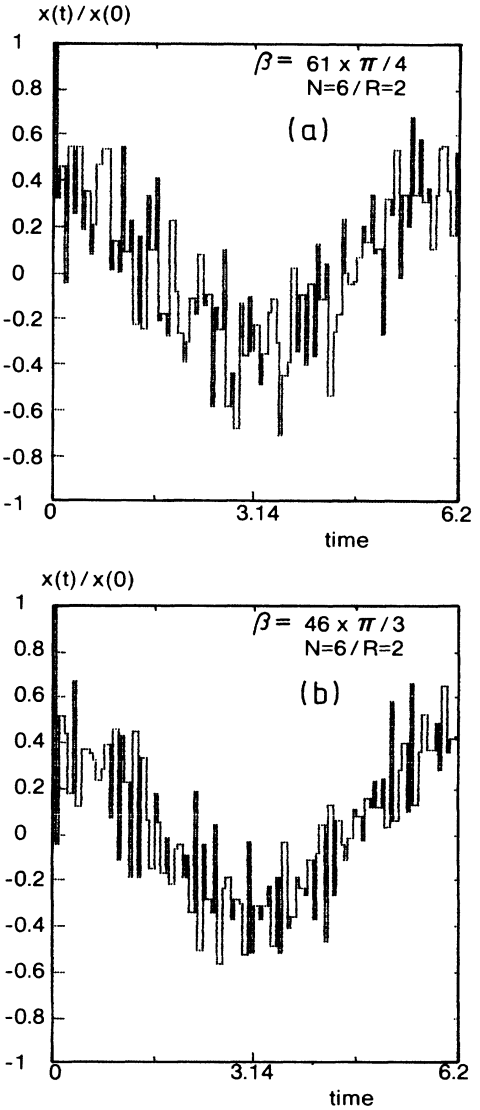

FIG. 5. Like Fig. 3, but for decreased $\Delta t=\pi/50$.

reduce to the well known single cosine function. Figure 4 also has the same legend as Fig. 2, but now for a doubled sampling frequency, so that $\Delta t = \pi/50$. This amounts to 101 sample points per figure along the time axis, which is getting close to the computer-graphics resolution (148 points in our case). Figure 5 represents a similar interpolation for Fig. 3. Comparing Figs. 2 and 4, or Figs. 3 and 5, exemplifies the earlier discussed rather deep difficulty in simply drawing a picture of $x(t)$. These features can be amplified by zooming towards, for instance, Fig. 3. Having decreased the sampling time interval by a factor $2^7 = 128$, i.e., from $\Delta t = \pi/25$ to $\Delta t = \pi/3200$, Fig. 6 shows a magnified portion of Fig. 3 (in this specific case, by choice, around $t = \pi$). Notice that the entire structure shown in Fig. 6 is completely unseen in Fig. 3. Next, in Fig. 7 we have again sampled the paths of Fig. 6, but with doubled accuracy, i.e., with 101 points so that $\Delta t = \pi/6400$.

At a second round of increased magnification, decreasing the sampling interval by another factor of $2^7 = 128$, from $\Delta t = \pi/3200$ to $\pi/409\,600$, Fig. 8 shows detail completely unseen in Fig. 6. Finally, Fig. 9 has the same legend as Fig. 8, but with the number of time samples again doubled from 51 to 101, so that now $\Delta t = \pi/819\,200$. That is, from Fig. 2 to Fig. 9 the sampling frequency varies over more than 4 orders of magnitude ($2^{15} = 32\,768$).

The details of such chaotic-looking pictures[25–28] as Figs. 2–9 are extremely sensitive to the precise values of β and the sampling instants. Of course, this sensitivity increases with increasing squeezing. For instance, computer samples of $x(t)$ at $R = 2$ at $\beta = 47.999\,99$ and $48.000\,01$ are virtually uncorrelated. This is also the case if, e.g., the initial sample time is shifted by the tiny amount of, say, $\delta t \approx 10^{-6}$. Such erratic features again indicate the almost nondifferentiable nature of $x(t)$. See further in Sec. III B.

Let it be recalled that even though the trajectories ap-

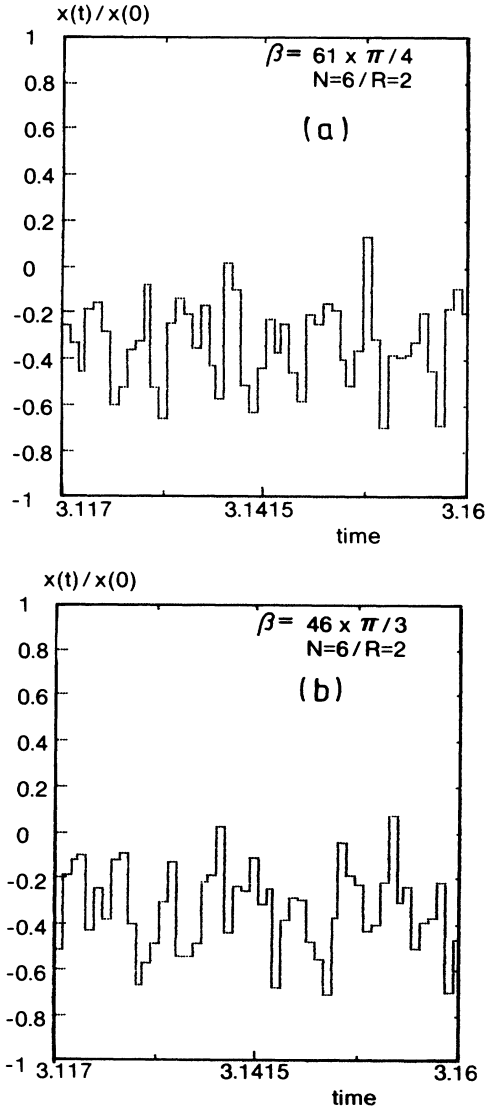

FIG. 6. Detail from the center of (but completely unseen in) Fig. 3. Here $\Delta t = \pi/3200$.

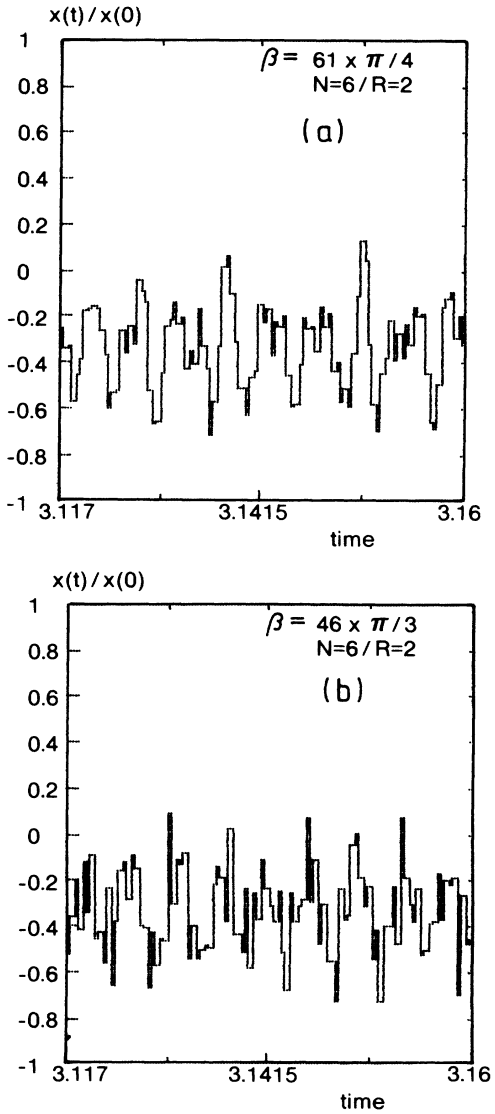

FIG. 7. Like Fig. 6, but for decreased $\Delta t = \pi/6400$.

parently come out quite noisy, they are basically deterministic functions given by the simple sum (3.1). In fact, if, for example, β (i.e., essentially the relative barrier height $U_0/\hbar\omega_0$) were only weakly fluctuating, the consequences for the details of the tunneling paths would be rather dramatic. However, there exists a more global characterization of $x(t)$ which is almost insensitive to β and the sampling instants, namely, its fractal (Hausdorff-Besicovitch-Mandelbrot[29,34]) dimension D, to be discussed in Sec. III B.

B. Fractal features

The successive figures of the preceding subsection apparently reveal ever more finer detail having roughly similar structure. Of course, as (3.1) is certainly not exactly self-similar (see below), this feature can only be approximate and valid over a restricted range of time scaling. Still, the plots already involve a range in time scale of the order of 10^5. Self-similarity (or at least, more general, self-affinity) is typical for fractal objects. Somewhat obscure until recently,[34] by now they seem to be almost omnipresent.[29,35–38] Well known examples of exact fractal curves are the Koch snowflake contour ($D=\ln 4/\ln 3\approx 1.2618$) and the "Peano monsters sweeps" ($D=2$). The standard stochastic fractal is the Brownian function ($D=1.5$). A classical natural fractal is the western coastline of Great Britain, which has $D\approx 1.25$ according to Richardson.[39]

Consider the real Weierstrass-Mandelbrot function[29,34,40]

$$\mathcal{R}\,W(t)\equiv \sum_{n=-\infty}^{\infty} w^n[1-\cos(\gamma^n t)]\ , \tag{3.5}$$

where $\gamma>1$ and $\gamma^{-1}<w<1$, and $\mathcal{R}$ denotes the real part.

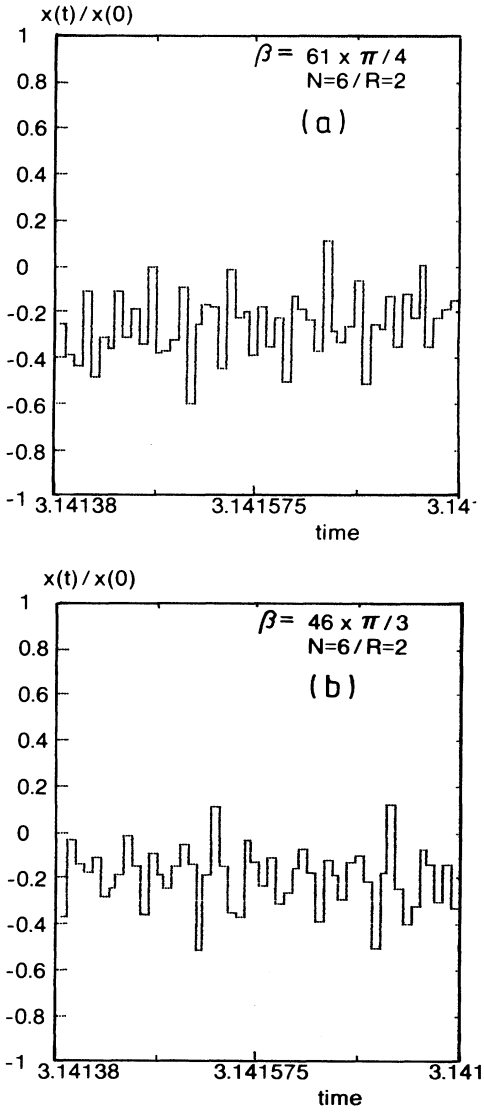

FIG. 8. Detail from the center of (but completely unseen in) Fig. 6. Now $\Delta t=\pi/409\,600$.

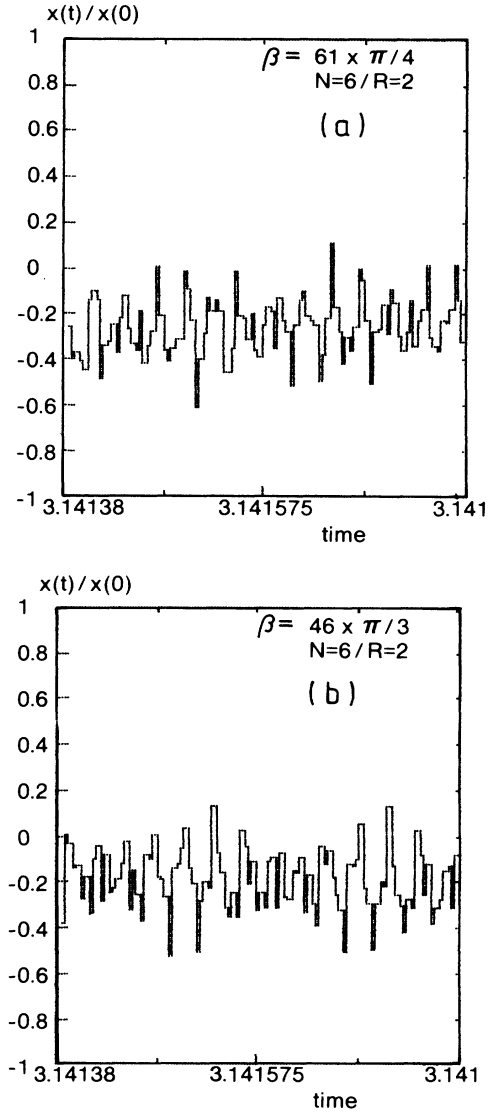

FIG. 9. Like Fig. 8, but for decreased $\Delta t=\pi/819\,200$.

This function is continuous but nowhere differentiable, and is easily shown to obey the scaling law

$$\mathscr{R}W(t/\gamma)=w\mathscr{R}W(t)\ . \tag{3.6}$$

That is, the function $\mathscr{R}W(t)$ is self-affine with respect to the focal time $t=0$ and the ratios w and γ^{-1}. In fact, it is exactly self-similar only if $w=\gamma^{-1}$. In general setting $w=\gamma^{D-2}$, it is claimed that D represents the curve's fractal dimension. A rigorous proof is highly nontrivial,[40] but the claim is easily understood as follows.

Let $y(t)$ be some function of time, and let $L(\Delta t)$ be the rectified length of $y(t)$ over a fixed period of time measured with increasingly finer "rulers" of length Δt. That is, $L(\Delta t)\equiv\sum|\Delta y|$ is the sum of all absolute increments $|\Delta y|$ traveled during each Δt. Then, according to Richardson's[39] general scaling law

$$L(\Delta t)/L(\Delta t_0)=(\Delta t/\Delta t_0)^{-\alpha}\ , \tag{3.7}$$

where $\alpha\equiv D-1$ is the excess dimension (with respect to the topological dimension, which is $D_T=1$ here), while D is the fractal dimension. As it should, if $D=D_T$ then $\alpha=0$ and upon increasing the time resolution $L(\Delta t)$ rapidly converges to a finite limit. Now let $y(t)=\mathscr{R}W(t)$, and let $\Delta t\equiv\gamma^{-m}$, $m\in\{n\}$, with $\Delta t_0\equiv\gamma^{-m_0}$. Hence, changing from Δt_0 to $\Delta t<\Delta t_0$, the number of sample points increases by the factor $\gamma^{m-m_0}>1$. On the other hand, according to the scaling law (3.6), the magnitude of $\mathscr{R}W(t)$ decreases by a factor w^{m-m_0} in this case. In effect, one expects $L(\Delta t)/L(\Delta t_0)=(\gamma w)^{m-m_0}$. Therefore, application of (3.7), i.e.,

$$\alpha=\ln[L(\Delta t)/L(\Delta t_0)]/\ln(\Delta t_0/\Delta t)\ , \tag{3.8}$$

yields $\alpha=1+\ln w/\ln\gamma$, which—being independent of m and m_0—means that $\mathscr{R}W(t)$ indeed is an exact fractal. inserting now $w\equiv\gamma^{D-2}$, readily leads to $\alpha=D-1$, which confirms the claim that D represents the fractal dimension of the Weierstrass-Mandelbrot function. The condition $\gamma^{-1}<w<1$, with $\gamma>1$, translates into $1<D<2$.

The function $\mathscr{R}W(t)$ is a generalized version of the original real Weierstrass function (note: the present prefactor differs from Ref. 29)

$$\mathscr{R}W_0(t)\equiv(1-w)\sum_{n=0}^{\infty}w^n\cos(\gamma^n t)\ , \tag{3.9}$$

again with $\gamma>1$ and $\gamma^{-1}<w<1$ in order to make $\mathscr{R}W_0(t)$ continuous but nondifferentiable. Notice that $\mathscr{R}W_0(0)\equiv 1$. This—at the time abhorrent—function was invented in 1872 as a counterexample to 19th century analysis.[29,34] Unlike (3.5) it is not generally scaling, but rather obeys

$$\mathscr{R}W_0(t/\gamma)-(1-w)\cos(t/\gamma)=w\mathscr{R}W_0(t)\ . \tag{3.10}$$

However, since according to (3.9) throughout $\mathscr{R}W_0(t)$ roughly varies between the values plus and minus one, letting $w\to 1$ does make (3.10) approach the form of the proper scaling law (3.6). That is,

$$\mathscr{R}W_0(t/\gamma)\approx w\mathscr{R}W_0(t)\ \text{ if } w\approx 1\ . \tag{3.11}$$

Consequently, again $D=2+\ln w/\ln\gamma$ which as $w\to 1$ implies $D\to 2$, an obviously sensible result. Actually, the formula for D when $w\approx 1$ is also easily grasped without reference to an explicit scaling law like (3.11), at least in the (within the present context) particularly relevant case $\gamma\gg 1$. Namely, if we let $\Delta t\equiv\theta\gamma^{-m}$ and $\Delta t_0\equiv\theta\gamma^{-m_0}$, respectively, with $\gamma^{-1}\ll\theta\lesssim\pi$, and if the respective amplitudes w^m and w^{m_0} are of the same order of magnitude, then $L(\Delta t)$ and $L(\Delta t_0)$ are essentially determined, respectively, by the modes with largely differing frequencies γ^m and γ^{m_0} so that one readily concludes $L(\Delta t)/L(\Delta t_0)\approx(\gamma^m/\gamma^{m_0})(w^m/w^{m_0})=(\gamma w)^{m-m_0}$. Hence, following (3.8) again $\alpha\approx 1+\ln w/\ln\gamma$.

Setting now $w\approx\tanh^2 R$ and $\gamma\approx\beta^2$ into (3.9), one obtains a form of the Weierstrass function, which is akin to the expected tunneling trajectory (3.1). Although the quantitative differences are obvious, the kinship is such that it serves to place the provoking pictorial features of Figs. 2–9 in an appropriate context, and $x(t)$ can be aptly called quasi-Weierstrassian. But then the tunneling trajectories may be expected to be natural (or quasi) fractals at least if $R\gtrsim 1$, i.e., for not too little squeezing of the initial wave packet. And since $\beta\gg 1$, the argument of the preceding paragraph valid for $\gamma\gg 1$ can be readily repeated here to obtain a formula for the dimension D. So, let $\Delta t\equiv\theta\Omega_m^{-1}$ and $\Delta t_0\equiv\theta\Omega_{m_0}^{-1}$, then $\Delta t_0/\Delta t=\Omega_m/\Omega_{m_0}$ and $L(\Delta t)/L(\Delta t_0)\approx(\Omega_m/\Omega_{m_0})(a_m/a_{m_0})$. Hence, by (3.8) $\alpha_{m,m_0}\approx 1+\ln(a_m/a_{m_0})/\ln(\Omega_m/\Omega_{m_0})$. Substituting then for the amplitudes (frequencies) the values from Eq. (3.2) [Eq. (3.3)], and setting $m\equiv m_0+1$, one may write the "differential" excess dimension as

$$\alpha_m\approx\ln\left[\left[\frac{\beta}{2m}\right]^2\tanh^2 R\right]\Big/\ln\left[\left[\frac{\beta}{2m}\right]^2\Big/\left[1-\frac{1}{2m}\right]\right]\ , \tag{3.12}$$

where $m=1,2,\ldots$. For example, with $\beta=48$ and $R=2$ one obtains $\alpha_1\approx 0.89$, $\alpha_2\approx 0.93$, $\alpha_3\approx\alpha_4\approx\alpha_5\approx 0.94$. Considering its derivation, (3.12) probably has its greatest significance if both $\beta\gg 1$ and $R\gg 1$. Letting R tend to zero, and recalling that $\alpha_m\geq 0$, one should define $\alpha_m\equiv 0$ whenever $R<\operatorname{arctanh}(2m/\beta)$. For $m=1$ and $\beta=48$ this yields $R<0.04$, which—if meaningful—indicates a rather rapid transition from smooth to fractal behavior. From here on we focus on α_1. Following Appendix B, a slightly more detailed analysis leads to the improved formula

$$\alpha_1=\ln[\tfrac{1}{2}\beta^2+(1-\tfrac{1}{2}\beta^2)/\cosh R]/\ln(\tfrac{1}{2}\beta^2)\ . \tag{3.13}$$

If $\beta\gg 1$ and $R\gg 1$, this yields $\alpha_1\approx 1-2e^{-R}/\ln(\frac{1}{2}\beta^2)$, while now $\alpha_1\approx\frac{1}{4}\beta^2R^2/\ln(\frac{1}{2}\beta^2)$ if $R\ll\beta^{-1}\ll 1$.

Because the tunneling paths are not exact fractals, the validity of the very concept should be verified numerically in this case. Therefore, along with the computations for the graphics of Figs. 2–9, the length $L(\Delta t)$ has been calculated, over one-half fundamental period, with the sampling time interval decreasing from $\Delta t_0=\pi/25$ to $\Delta t=\pi/409\,600$. For intervals $\pi/10\lesssim\Delta t\lesssim\pi$, the length was found to fluctuate around a constant value, roughly $2a_0$, as expected. Samples have been taken from half-periods around $t=\pi$, 3π, and 5π. For the higher sampling frequencies it became prohibitive to actually sample

the entire half-period, so only a portion of it was taken and the ensuing lengths were upscaled accordingly. This upscaling has been done linearly in the ratio of π relative to the actual period of time, correcting for the feature that if $\Omega_n \Delta t \ll 1$, the $\cos(\Omega_n t)$ term is sampled in detail only over a part of one of its half-periods rather than over (one or more) full half-periods and, hence, that the pertinent contribution to the total length should be upscaled goniometrically rather than linearly. Actually, for all significant values of the squeezing $R \gtrsim 0.5$ (and at $\beta \approx 48$)—and also in view of the sufficiently large range of sampling frequencies—these corrections hardly influenced the resulting values of the fractal dimension.

The excess dimension $\alpha(R)$ has been determined by (3.8) for $R=0.5$, 1, 1.5, and 2, with (a) $\beta=61\pi/4 \approx 47.9093$ and (b) $\beta=46\pi/3 \approx 48.1711$. Within the estimated accuracy for α of a few percent, the fractal dimensions for these two β values were identical. In fact, Figs. 10—13 are based on averages of the data [for $\ln(L/L_0)$, not for L/L_0 itself, to be sure] for (a) and (b). The straight lines shown in the figures are calculated by means of the standard method of least squares.[41,42] In particular, the excellent fit of the sample points to the straight line for $R=2$ appears to confirm the significance

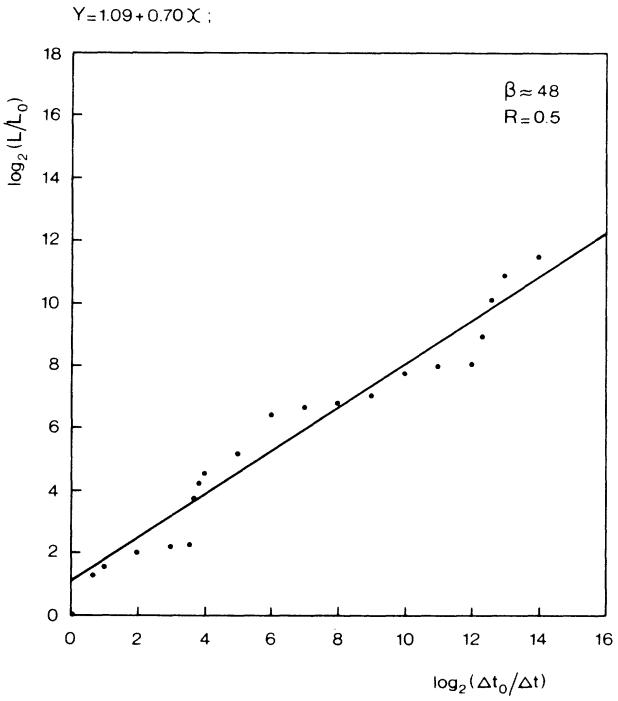

FIG. 10. Fractal analysis of the expected normalized position as a function of time, for a particle tunneling in a symmetric bistable potential. Squeezing parameter $R=0.5$; $\beta \approx 48$; $L(\Delta t)$ is the rectified sampled length covered during a fixed period of time [here actually equal to π, so that $L(\Delta t_0) \approx 2$ with $\Delta t_0 = \pi/25$]. Note that the sampling frequency varies over more than 4 orders of magnitude ($2^{14}=16384$). The slope of the least-squares straight line through the computer data equals the excess dimension (or Richardson's parameter) $\alpha \approx 0.70$ [theoretical value $\alpha_1 \approx 0.69$ according to (3.13)], which implies a fractal (or Hausdorff-Besicovitch-Mandelbrot) dimension $D \approx 1.70$.

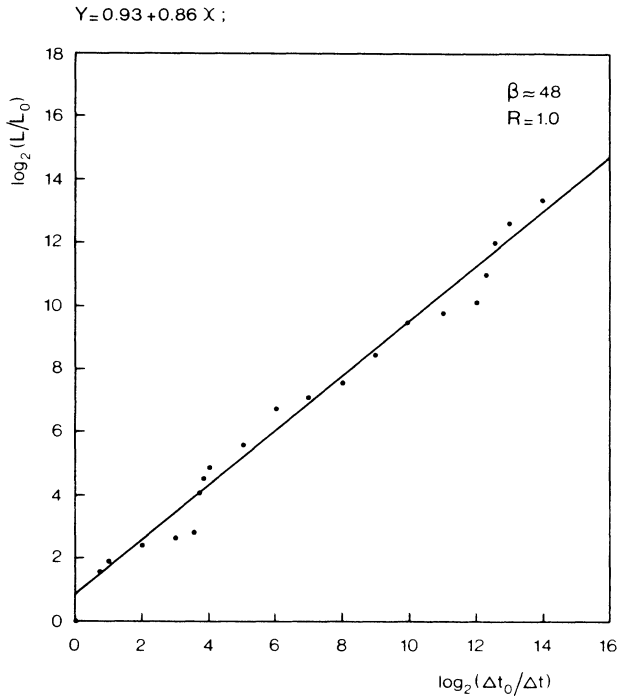

FIG. 11. Like Fig. 10, but for $R=1$. Here $\alpha \approx 0.86$ (while $\alpha_1 \approx 0.85$ now), so that $D \approx 1.86$.

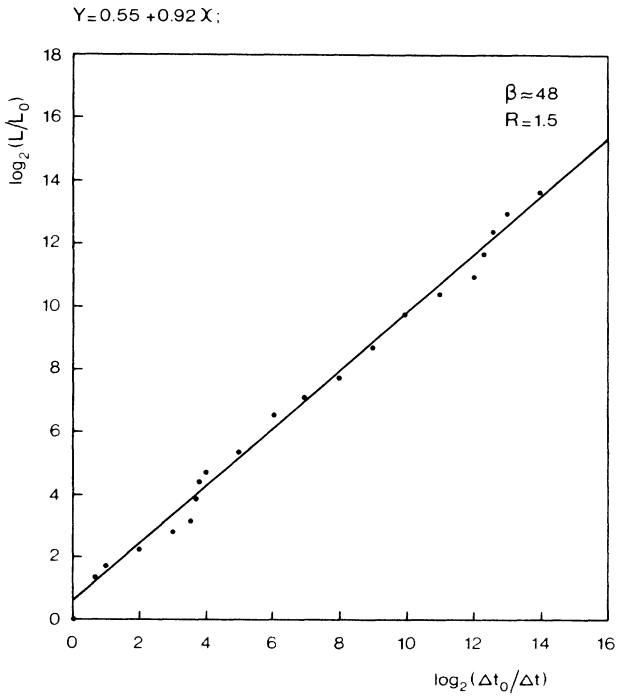

FIG. 12. Like Fig. 10, but for $R=1.5$. Now $\alpha \approx 0.92$ ($\alpha_1 \approx 0.92$ too), so that $D \approx 1.92$.

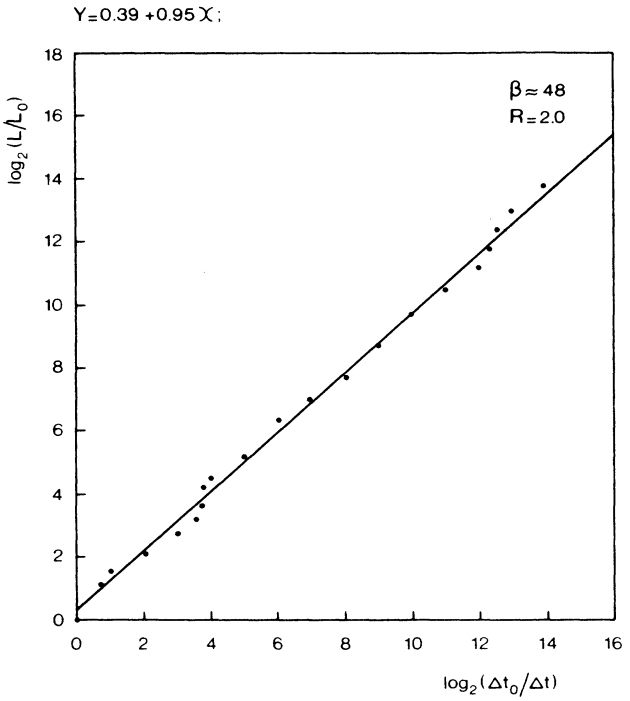

FIG. 13. Like Fig. 10, but for $R=2$. In this case $\alpha\approx 0.95$ (also $\alpha_1\approx 0.95$), so that $D\approx 1.95$.

of the fractal nature of the squeezed wave packet's tunneling trajectory.

The observed structure, more apparent for lower R, namely that the data are clearly below (above) the straight line if $\log_2(\Delta t_0/\Delta t)$ is less (greater) than approximately 3.5 may be explained as follows. At $\log_2(\Delta t_0/\Delta t)=3$ one has $\Delta t=\pi/200$, so that, with $\beta=48$, both $\Omega_1\Delta t\approx 6\pi$ and $\Omega_2\Delta t\approx 1106\pi$ are even multiples of π. In consequence, samples being almost in phase, the contributions to the rectified length are small. On the other hand, at

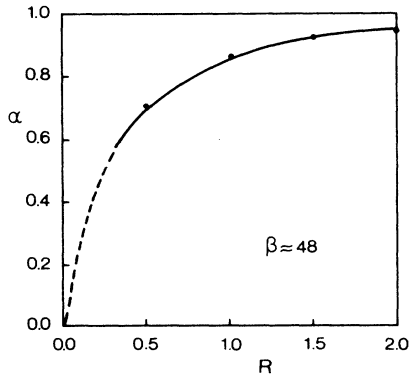

FIG. 14. Excess fractal dimension $\alpha\equiv D-1$ as a function of squeezing. The dots at $R=0.5$, 1, 1.5, and 2 represent the computer data from Fig. 10—13. The line is $\alpha_1(R)$ according to (3.13). The theoretical curve has been dashed as it tends to the origin $\alpha_1(0)=0$ because its significance decreases in this limit. Since upon squeezing rapidly $\alpha>0.5$, so that $D>1.5$, the tunneling trajectories have a strong tendency to become antipersistent (Ref. 29).

$\log_2(\Delta t_0/\Delta t)=4$ one has $\Delta t=\pi/400$, and both $\Omega_1\Delta t\approx 3\pi$ and $\Omega_2\Delta t\approx 553\pi$ are odd multiples of π, which leads to relatively large contributions to $L(\Delta t)$. In addition, at $\Delta t=\pi/300$, i.e., $\log_2(\Delta t_0/\Delta t)\approx 3.6$, one has $\Omega_1\Delta t\approx 4\pi$ but $\Omega_2\Delta t\approx 737\pi$, clearly an intermediate case. Similar remarks concern the structure at $\log_2(\Delta t_0/\Delta t)\approx 12.5$.

Finally, Fig. 14 represents the data for the fractal excess dimension $\alpha(R)\equiv D(R)-1$ as a function of the squeezing parameter R. It is recalled that α only depends on the absolute value of R. The solid line in Fig. 14 is a straightforward plot of the theoretical value α_1 according to (3.13). In fact, the near coincidence of the data points and the theoretical prediction is far better than could be hoped for. In view of the lessening significance of the fractal dimension for decreasing R, the portion of the theoretical curve extending to $R=0$ has been dashed.

IV. CONCLUSIONS

In this paper the following has been achieved.

First, an explicit and simple formula has been derived for the exponentially small energy-level splittings $\Delta E_{2n}\equiv E_{2n+1}-E_{2n}$ (with $n=0,1,\ldots$) for both the ground state ($n=0$) and the excited-state ($n\geq 1$) doublets in a symmetric bistable potential $U(x)$. This potential has parabolic minima at $x=\pm a$ [where $U(x)\approx\frac{1}{2}\omega_0^2(x\pm a)^2$], separated, by an arbitrarily shaped barrier with height $U_0\gg\hbar\omega_0$. See Fig. 1. The exponential prefactor (or attempt frequency $\bar{\omega}_{2n}$ improves on the semiclassical value and generalizes the instanton-method result for the ground-state doublet to $n\neq 0$.

Second, using the obtained spectrum, the tunneling propagator is constructed. In particular, the expected position $x(t)$ of an initially squeezed Gaussian wave packet, located at $t=0$ in a potential well, is determined as a coherent superposition of cosine functions of time. In the absence of squeezing ($R=0$) only the ground-state doublet cosine survives, which yields the standard example of molecular inversion.

Third, it is shown that the simple question for a drawing of the expected position versus time does not have a simple answer. For $R\neq 0$ the sampled trajectories behave rather erratically, the details sensitively depending on, for example, the barrier height ($\beta\sim U_0/\hbar\omega_0$) and the precise sampling instants. Although the trajectory is basically deterministic, it looks noisy. Zooming towards the pictures, by decreasing the time scale over more than 4 orders of magnitude (namely, $2^{15}=32\,768$), reveals ever more virtually similar but previously unseen structure.

Fourth, these provoking characteristics are shown to arise from the quasi-Weierstrassian nature of the tunneling spectrum. By means of an argument involving the exact affine scaling Weierstrass-Mandelbrot fractal function, a formula is derived for the approximate fractal (Haussdorff-Besicovitch-Richardson) dimension D of $x(t)$, as a function of R and β. This theoretical formula is successfully tested against numerical data by computing the rectified sample length $L(\Delta t)$ of $x(t)$. For example, at $R=2$ this length varies from $L(\pi/25)\approx 2$ to $L(\pi/819\,200)\approx 10^5$. The final result is shown in Fig. 14.

Inter alia, arguments are given (i) for a simple "deriva-

tion" of semiclassical tunneling frequencies (in Sec. I), (ii) for a heuristic "proof" of the fractal nature of the Weierstrass-Mandelbrot function (in Sec. III B), and (iii) in favor of a particular shape of the ammonia molecule's double-well potential barrier (in Appendix A).

ACKNOWLEDGMENTS

I am particularly grateful to Dr. J. A. Boden for his generous assistance in the numerical calculations.

APPENDIX A: THE AMMONIA MOLECULE

It will be useful to gauge the numerical validity of the splitting formulas (2.14)—(2.16) for higher doublets in a realistic example. To this end let us briefly discuss the NH_3 molecule and consider the pertinent data $\omega_0=1.79\times10^{14}$ s^{-1}, $\Delta\omega_0=0.15\times10^{12}$ s^{-1}, $\Delta\omega_2=6.4\times10^{12}$ s^{-1}, and $2a=0.76\times10^{-10}$ m (see Refs. 3 and 14). Introducing the reduced nitrogen mass $m\neq1$ into the formulas, one infers that $\exp(\omega_0\tau_0)=(\hbar\Delta\omega_2/2ma^2\omega_0\Delta\omega_0)^{1/2}\approx0.60(m_0/m)^{1/2}$, where m_0 is the free nitrogen mass (i.e., $m_0=14m_p$, $m_p=1.67\times10^{-27}$ kg being the proton mass). Invoking the appropriate ratio $m_0/m=\frac{17}{3}$, the result reads $\exp(\omega_0\tau_0)\approx1.43$, which is quite an acceptable value remembering that $\exp(\omega_0\tau_0)=1$ for the double harmonic oscillator[1,22] and knowing[22] that $\exp(\omega_0\tau_0)=2$ for the quartic potential $U(x)\equiv\frac{1}{8}(\omega_0/a)^2(x^2-a^2)^2$. Even better, for the equally simple potential $U(x)\equiv U_0\cos^2(\pi x/2a)$ on $|x|\leq a$, one has $\exp(\omega_0\tau_0)=4/\pi\approx1.27$. Using the above formula for $\exp(\omega_0\tau_0)$, one may obtain $\exp(-S_0/\hbar)=[\pi(\Delta\omega_0)^3/2\omega_0^2\Delta\omega_2]^{1/2}\approx1.61\times10^{-4}$. Hence, $S_0/\hbar\approx8.73$. Since for typical analytic barriers one has $S_0=f_0ma^2\omega_0$, where f_0 is a specific barrier form factor, we determine $f_0\approx8.73\hbar/ma^2\omega_0\approx0.86$ for NH_3. Comparing this with the values $f_0=1$ for the double oscillator, $f_0=2/3\approx0.67$ for the quartic potential and $f_0=8/\pi^2\approx0.81$ for the cosine-squared potential, it is confirmed that the latter indeed seems to provide an appropriate elementary representation of the ammonia double-well system. It is then finally of interest to note that since for this particular barrier $U_0=2ma^2\omega_0^2/\pi^2$, while the mean energy for the excited doublet is given by $E_2\approx3\hbar\omega_0/2$, one finds the rather large ratio $E_2/U_0\approx3\pi^2\hbar/4ma^2\omega_0=6\hbar/S_0\approx0.69$.

APPENDIX B: THE FRACTAL DIMENSION

The derivation of the excess dimension (3.13) proceeds as follows. Let $\Delta t_0\equiv\theta\Omega_0^{-1}$ and $\Delta t_1\equiv\theta\Omega_1^{-1}$, with $\theta\lesssim\pi$, and let the rectified sample lengths (for definiteness, over one-half fundamental period) be written as

$$L(\Delta t_0)\approx2a_0\eta_0(\Delta t_0)+2a_1\eta_1(\Delta t_0)+\cdots,$$
$$L(\Delta t_1)\approx2a_0\eta_0(\Delta t_1)+2a_1\eta_1(\Delta t_1)+\cdots, \tag{B1}$$

where a_n has been given in (3.2) and where $\eta_n(\Delta t)$ is a measure of the efficiency with which the nth mode is being sampled at intervals Δt. This efficiency is most easily defined as the product

$$\eta_n(\Delta t)\equiv N_n\mu_n(\Delta t)\nu_n(\Delta t), \tag{B2}$$

where $N_n\approx\Omega_n/\Omega_0$ essentially counts the number of half-periods of the nth mode that fit into a fundamental half-period. Hence, $\mu_n(\Delta t)$ and $\nu_n(\Delta t)$ can be taken to concern only one nth-mode half-period.

Now let $\mu_n(\Delta t)$ be the probability that a particular half-period of mode n is being sampled at least once. So, $\mu_n(\Delta t)$ is a fraction between zero and one. Roughly speaking if $\Omega_n\Delta t\gg1$ than $\mu_n(\Delta t)\approx\pi/\Omega_n\Delta t$, while if $\Omega_n\Delta t\lesssim\pi$ one has $\mu_n(\Delta t)\approx1$. Then, finally, $\nu_n(\Delta t)$ is concerned with a surely sampled half-period of the nth mode. If there were just one sampling (at a randomly distributed instant), then the mean length contribution for this mode would amount to $2a_n/\pi$ (rather than the full $2a_n$). Therefore, $\nu_n(\Delta t)\approx1/\pi$ in this case. On the other hand, if $\Omega_n\Delta t\lesssim\pi$ then $\nu_n(\Delta t)\approx1$.

With the present values for Δt_0 and Δt_1, one thus finds $\mu_0(\Delta t_0)\approx1$, while $\mu_{n>0}(\Delta t_0)\approx\pi/\Omega_n\Delta t_0$; and $\nu_0(\Delta t_0)\approx1$, while $\nu_{n>0}(\Delta t_0)\approx1/\pi$. Further, $\mu_0(\Delta t_1)\approx\mu_1(\Delta t_1)\approx1$, but $\mu_{n>1}(\Delta t_1)\approx\pi/\Omega_n\Delta t_1$; and $\nu_0(\Delta t_1)\approx\nu_1(\Delta t_1)\approx1$, but $\nu_{n>1}(\Delta t_1)\approx1/\pi$. Hence, (B1) yields

$$L(\Delta t_0)\approx2a_0+(2/\theta)\sum_{n=1}^{\infty}a_n,$$
$$L(\Delta t_1)\approx2a_0+(\beta^2/\theta)\sum_{n=1}^{\infty}a_n, \tag{B3}$$

where we have accounted for $\Omega_0\equiv1$, $\Omega_1=\frac{1}{2}\beta^2$, and where $\theta\lesssim\pi$. Employing now the normalization of (3.1) at $t=0$, i.e., $\sum_{n=1}^{\infty}a_n=1-a_0$, and inserting the educated choice $\theta\approx1$, (B3) considerably simplifies and leads to

$$L(\Delta t_1)/L(\Delta t_0)\approx\tfrac{1}{2}\beta^2+(1-\tfrac{1}{2}\beta^2)a_0. \tag{B4}$$

Now taking $a_0=1/\cosh R$ from (3.2), and recalling that $\Delta t_0/\Delta t_1=\Omega_1=\frac{1}{2}\beta^2$, and inserting (B4) into (3.8), one readily obtains the upshot (3.13) for the excess dimension α_1.

[1]E. Merzbacher, *Quantum Mechanics* (Wiley, New York, 1970), p. 70.
[2]H. Dekker, Physica **103A**, 55 (1980).
[3]D. M. Dennison and G. E. Uhlenbeck, Phys. Rev. **41**, 313 (1932).
[4]C. H. Townes and A. L. Schawlow, *Microwave Spectroscopy* (McGraw-Hill, New York, 1955).
[5]M. Simonius, Phys. Rev. Lett. **40**, 980 (1978).
[6]A. J. Leggett, Prog. Theor. Phys. Suppl. **69**, 80 (1980).
[7]R. de Bruyn Ouboter, in *Proceedings of the International Symposium on the Foundations of Quantum Mechanics,* edited by S. Kamefuchi (Physical Society of Japan, Tokyo, 1984), p. 83.
[8]L. D. Landau and E. M. Lifshitz, *Quantum Mechanics* (Pergamon, London, 1958), p. 174.
[9]L. I. Schiff, *Quantum Mechanics* (McGraw-Hill, New York, 1968).

[10]S. Chakravarty and A. J. Leggett, Phys. Rev. Lett. **52**, 5 (1984).
[11]D. W. Bol. J. J. F. Scheffer, W. T. Giele, and R. de Bruyn Ouboter, Physica **133B**, 196 (1985).
[12]A. J. Leggett and A. Garg, Phys. Rev. Lett. **54**, 857 (1985).
[13]H. Dekker, Phys. Rev. A **35**, 1436 (1987).
[14]R. P. Bell, *The Tunnel Effect in Chemistry* (Chapman and Hall, London, 1980).
[15]S. Coleman, in *The Whys of Subnuclear Physics,* edited by A. Zichichi (Plenum, New York, 1979), p. 805.
[16]J. S. Langer, Ann. Phys. (N.Y.) **41**, 108 (1967).
[17]A. M. Polyakov, Nucl. Phys. **B121**, 429 (1977).
[18]C. Callan and S. Coleman, Phys. Rev. D **16**, 1762 (1977).
[19]C. Milburn and D. F. Walls, Opt. Commun. **39**, 401 (1981).
[20]D. F. Walls, Nature **306**, 141 (1983).
[21]M. Wolinsky and H. J. Carmichael, Opt. Commun. **55**, 138 (1985).
[22]H. Dekker, Phys. Lett. **114A**, 295 (1986).
[23]R. P. Feynman and A. R. Hibbs, *Quantum Mechanics and Path Integrals (McGraw-Hill, New York, 1965).*
[24]H. Dekker, in *Functional Integration: Theory and Applications,* edited by J. P. Antoine and E. Tirapequi (Plenum, New York, 1980), p. 207.
[25]J. Ford, Phys. Today **36** (April), 1 (1983).
[26]L. P. Kadanoff, Phys. Today **36** (December), 46 (1983).
[27]P. Bergé, Y. Pomeau, and Ch. Vidal, *L'Ordre dans le Chaos* (Hermann, Paris, 1984).
[28]G. Casati, *Chaotic Behaviour in Quantum Systems* (Plenum, New York, 1985).
[29]B. B. Mandelbrot, *The Fractal Geometry of Nature* (Freeman, New York, 1983).
[30]*Table of Integrals, Series and Products,* edited by I. S. Gradshteyn and I. M. Ryzhik (Academic, New York, 1980).
[31]H. Dekker, Phys. Rev. A **24**, 3182 (1981).
[32]*Handbook of Mathematical Functions,* edited by M. Abramowitz and I. A. Stegun (Dover, New York, 1972).
[33]G. Szegö, *Orthogonal Polynomials* (American Mathematical Society, Providence, 1975).
[34]B. B. Mandelbrot, *Fractals: Form, Chance, and Dimension* (Freeman, San Franciso, 1977).
[35]L. Pietronero, *Fractals in Physics* (Elsevier, Amsterdam, 1986).
[36]J. G. Powles and N. Quirke, Phys. Rev. Lett. **52**, 1571 (1984).
[37]S. Tsurumi and H. Takayasu, Phys. Lett. **113A**, 449 (1986).
[38]S. Toxvaerd, Phys. Lett. **114A**, 159 (1986).
[39]L. F. Richardson, General Systems Yearbook **6**, 139 (1961), especially Sec. 7.
[40]M. V. Berry and Z. V. Lewis, Proc. R. Soc. London Ser. A **370**, 459 (1980).
[41]M. R. Spiegel, *Theory and Problems of Statistics* (Schaum, New York, 1961).
[42]A. Papoulis, *Probability, Random Variables and Stochastic Processes* (McGraw-Hill, Tokyo, 1965).